ORIGINAL PAPER

Modelling excess surface energy in dry and wetted calcite systems

Bjørn Kvamme · Tatyana Kuznetsova · Daniel Uppstad

Abstract   We have combined the calcite force field of Hwang et al. (J. Phys. Chem. B 105:4,122–4,127, 2001) with the F3C water model and a hybrid Lennard-Jones/van der Waals 3-site potential for CO_2 to investigate the $(10\bar{1}4)$ and $(10\bar{1}0)$ cleaving surfaces of calcite under dry and wetted conditions. The wetting fluid included both pure water and water–carbon dioxide mixture. Excess surface energies and structural features of the calcite–fluid interface were analyzed, with the simulation results for the relaxed surfaces confirming the experimentally observed morphology and supporting our conclusion that the relative stability order of calcite cleaving surfaces under investigation will remain unchanged in the presence of water–carbon dioxide mixture as well.

Keywords   Calcite · Carbon dioxide · Water · Molecular modeling

1 Introduction

Calcium and magnesium carbonates are the most abundant within the rhombohedral carbonate mineral family, which comprises 4% of the earth's crust. A detailed understanding of mechanisms and phenomena governing precipitation and dissolution of calcium carbonate is therefore essential to predict the processes taking place when this mineral comes into a contact with either pure water or aqueous solutions. Molecular simulations are a promising complimentary tool offering molecular-level insights into the separate components of the complex experimental processes and often capable of providing explanations and predictions at observational scales. We present molecular dynamics investigation for the two most stable calcite surfaces under dry and wetted

B. Kvamme (✉) · T. Kuznetsova · D. Uppstad
Department of Physics, University of Bergen, Allègt. 55, 5007 Bergen, Norway
e-mail: bjorn.kvamme@ift.uib.no

conditions. The wetting phase comprised both pure water and water–carbon dioxide mixtures.

2 Computational methods

2.1 Simulation protocol

The molecular dynamics used constant-temperature, constant-pressure algorithm from MDynaMix package of Lyubartsev and Laaksonen [5]. The starting interfacial system was constructed from slabs of bulk water–carbon dioxide mixture and appropriately cleaved calcite crystal, thermalized initially at 298 K and set side by side, with the periodic boundary conditions applied. The resulting systems (described in Table 1) were subsequently equilibrated for several tens of picoseconds before the average collection began. The production time amounted to 200 picoseconds. Time step was set to 10^{-16} s to allow for accurate integration of internal degrees of freedom. The system was kept at constant temperature of 298 K. Electrostatic interactions were handled by the Ewald summation technique with a variable number of reciprocal vectors. Linux-based message passing interface (MPI) was used to implement parallel computation on a cluster dual-processor machines. The number of processors ranged from 2 to 12. Cut-off radius for the Lennard-Jones potential and electrostatic forces was 12 Å. Six different systems were simulated; system details are stated in Table 1 below. The calcite crystal was cleaved along the $(10\bar{1}0)$ plane in systems 3, 4 and 5. System 6, on the other hand, had the $(10\bar{1}4)$ plane facing the water–CO_2 interface.

2.2 Molecular force fields

The 3-site F3C water model of Levitt et al. [4] (with SPC/E charges since we found that the original ones gave a worryingly flat RDF) was used in the simulations. The model is 3-site, and differ from the majority of water force fields in that its hydrogens possess a small amount of van der Waals interaction useful to offset the otherwise unshielded Coulombic attraction between positively charged water hydrogens and calcite anions.

For modeling calcite, we used a combination of two molecule models; a 1-site model for the Ca^{2+} ion and a 4-site model for the CO_3^{2-} ion. Both models were adopted from

Table 1 Simulated systems

System	Box lengths (Å)	Number of molecules
1	$24.4 \times 25.0 \times 29.0$	588 H_2O, 19 CO_2
2	$17.1 \times 20.0 \times 29.3$	330 H_2O, 11 CO_2
3	$17.1 \times 20.0 \times 49.3$	96 Ca^{2+}, 96 CO_3^{2-}, 330 H_2O, 11 CO_2
4	$17.1 \times 20.0 \times 49.3$	96 Ca^{2+}, 96 CO_3^{2-}, 330 H_2O, 11 CO_2
5	$17.1 \times 20.0 \times 49.3$	96 Ca^{2+}, 96 CO_3^{2-}, 330 H_2O, 11 CO_2
6	$24.4 \times 25.0 \times 49.0$	240 Ca^{2+}, 240 CO_3^{2-}, 588 H_2O, 19 CO_2

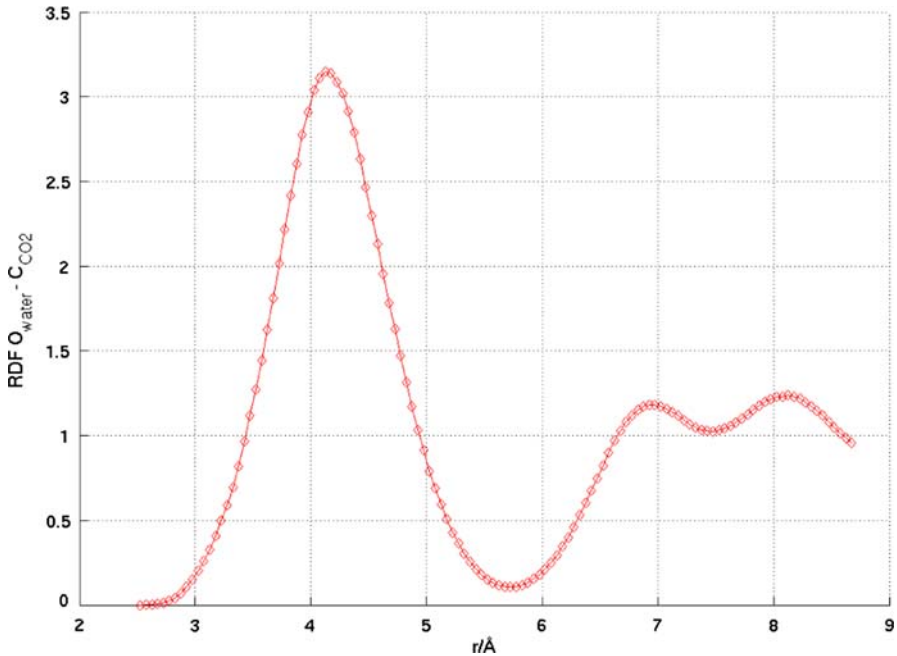**Fig. 1** Radial distribution functions of water oxygen–carbon dioxide carbon under the same conditions as Panhuis et al. [7]

Hwang et al. [2]. The ζ, R_0, D_0 exp-6 parameters were fitted Mayo et al. [6] to yield accurate lattice parameters.

The water–CO_2 interactions used a 3-site Lennard-Jones model carbon dioxide model of Panhuis et al. [7], well suited to describe the behavior of isolated CO_2 molecules in water. As for CO_2–calcite and CO_2–CO_2 interactions, we modified the original 5-site CO_2 model due to Tsuzuki et al. [8] by merging the van der Waals and Coulombic interaction sites to make it into a 3-site one. The charges were also exchanged for those of Panhuis et al. [7]. We tested the validity of combining these force fields by comparing radial distribution functions (RDFs) of systems 1 and 2 (Table 1) for water oxygen–CO_2 oxygen and water oxygen–CO_2 carbon with the findings of Panhuis et al. [7]. Our RDFs (Fig. 1) matched those of Panhuis et al. [7] quite well.

2.3 Density profiles

The density profiles of $x - y$ averaged quantities of interest were generated by partitioning the simulation box into discrete bins in the z direction. The atomic density profile for atom of type i was thus obtained by

$$\langle \rho_i(z) \rangle = \frac{\langle m_i N_i(z) \rangle}{A \Delta z} \tag{1}$$

where N_i is the number of i-type atoms in a slab located between z and $z + \Delta z$, A is the cross-section area, $A = L_x L_y$, m_i is the atom's mass, Δz, the slab's width.

Varying the binning width in 0.095–0.475 Å range (1800–360 bins) did not affect the profiles in any significant way.

3 Results and discussion

Findings reached in this work are not directly comparable to either experimental or modelling results, since nobody (to our knowledge) has performed either experiments or numerical simulations involving calcite in contact with water–CO_2 mixture. This is why the validity of our approach was tested on calcite–water systems. Two calcite surfaces ($10\bar{1}4$ and $10\bar{1}0$) were investigated to see which surface had the lowest surface energy. Both experimental results and simulations state that the $(10\bar{1}4)$ surface is the most stable one under both dry and wet conditions (corresponds to the lowest surface energy). Our results for pure water and calcite and calcite in vacuum showed a good qualitative agreement with (wildly varying) results of previous numerical treatment of other authors, as well a good quantitative agreement with the work of Hwang et al. [2] (results of others summarized in Table 2). The best agreement was with Hwang et al. [2] due their model being used and their approach followed, though with modifications (cross-interactions). The differences between wet and dry surface energies were also consistent. If the mineral is water-wet, the excess energy should be significantly lower for the hydrated surface compared to that of dry surface. This can be cited as the second point of agreement.

The next step was to investigate how adding CO_2 to the water would affect the excess surface energies of the two calcite–liquid surfaces under study ($10\bar{1}4$ and $10\bar{1}0$).

Excess surface energy, γ, a good indicator of the relative stability of surfaces, as well as the strength of hydration, is presented in Table 3.

$$\Delta E = E_{\text{interface}} - E_{\text{bulk}} - E_{\text{water}}, \tag{2}$$

Table 2 Comparison of excess surface energies of calcite–water and calcite–water–CO_2 systems reported by various researchers and this work

Surface	Reference	Excess energy, J/m^2	
		$\{10\bar{1}4\}$	$\{10\bar{1}0\}$
Dry	This work	0.860	1.500
	Hwang et al. (model used) [2]	0.863	1.37
	Wright et al. [9]	0.322	–
	Kerisit et al. [3]	0.59	0.95
Wet (pure water)	This work	0.288	0.778
	Hwang et al. (model used) [2]	0.232	–
	Wright et al. (water monolayer) [9]	0.21	0.72
	Kerisit et al. [3]	0.387	–
Wet (aqueous CO_2)	This work	0.419	0.794

Table 3 Excess surface energies and potential energies for calcite–water–CO_2 systems

System	Box lenghts (Å)			Potential energy per 'particle' (kJ/mol)	Excess surface energy (J/m^2)
	x	y	z		
1	24.4	25.9	29.0	-43.0770 ± 0.0009	–
2	17.1	20.0	29.3	-42.9560 ± 0.0018	–
3	17.1	20.0	49.3	-544.1338 ± 0.0006	0.79 (4)
4	17.1	20.0	49.3	-544.1621 ± 0.0008	0.79 (0)
5	17.1	20.0	49.3	-544.1293 ± 0.0006	0.79 (4)
6	24.4	25.9	49.0	-662.2044 ± 0.0005	0.41 (9)

$$\gamma_{\text{interface}} = \frac{\Delta E}{(2A_s N_A)}, \tag{3}$$

where E is system's total potential energy, A_s is surface area, N_A, the Avogadro number.

The difference in surface energy, $\Delta \gamma$, between the most stable and the next most stable calcite surfaces amounted to

$$\Delta \gamma = \gamma_{(10\bar{1}0)} - \gamma_{(10\bar{1}4)} = (0.794 - 0.419)\,\text{J/m}^2 = 0.375\left(\text{J/m}^2\right) \tag{4}$$

Excess surface energies of surfaces wetted by the mixture of water and CO_2 retain the relative stability order. That is the $(10\bar{1}4)$ surface still clearly has the lowest excess energy (0.794 J/m^2). It is by 0.375 J/m^2 lower than in the $(10\bar{1}0)$ surface (0.419 J/m^2), indicating that the $(10\bar{1}4)$ surface is still the most stable one energetically. However, it does appear that the increase in excess surface energy associated with the addition of carbon dioxide is larger for the stable $(10\bar{1}4)$ surface.

There are several instructive features to be observed in the density profiles (see Fig. 3). First, the average water densities show distinctive peaks at each side of the crystal. Both the relatively low first peak on the right-hand side and the almost non-existent one on the left can be explained by "ridges" characteristic for the calcite surface effectively decreasing the net projected density. It is thus the enhanced density of the second and the third water layers compared to that of bulk water that will truly reflect the affinity of water affinity for the calcite surface.

Second, a closer look at the calcite crystal will show that density peaks corresponding to different calcite constituent atoms are aligned within the crystal bulk but shifted relative to each other in the interfacial layers. In the layer closest to the interface, one can see that the oxygen and calcium peaks lie closer to the interface than those of carbon. This is probably due to positively charged calcium ion interacting significantly with the oxygen in water, and the carbonate oxygen attracted by water hydrogen. This is the origin of the excess energy. In the second layer from the interface, the calcium cation is still positioned closer to the interface than the carbon, but the oxygen peak has moved to the other side of the carbon peak. This is probably a consequence of the disorder in the first layer.
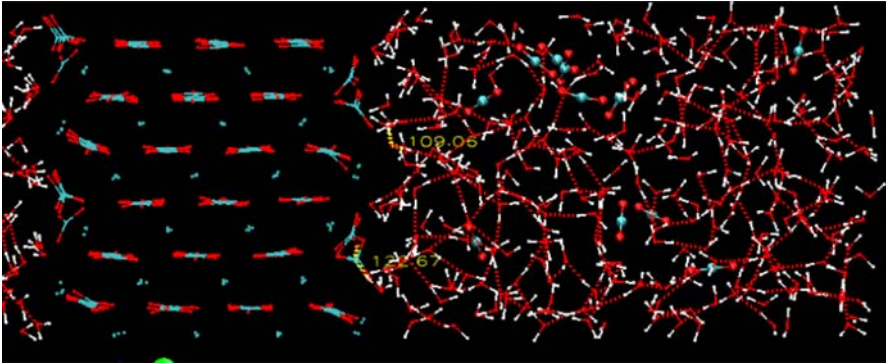
Fig. 2 VMD package [1]—generated presentation of simulation system 4 $\{10\bar{1}0\}$ cleaving plane. Water–carbon dioxide mixture on the *right-hand side*
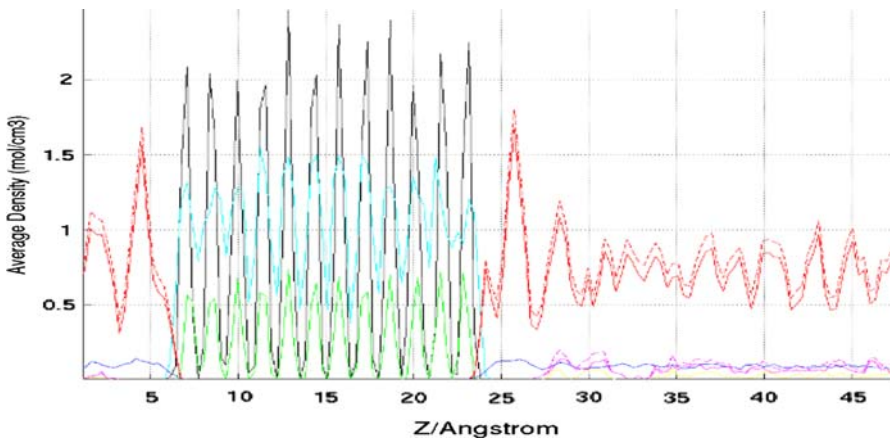

Fig. 3 Density profiles of simulation system 4. *Full red line* is water oxygen; *blue*—water hydrogen; *dashed red line* indicates total water density profile; *yellow* is the carbon (C) in CO_2; *purple* is the oxygen (O) in CO_2; *black* is calcite calcium cation; *cyan*—oxygen (O) of the calcite carbonate anion; *green*—carbon (C) of the calcite carbonate anion

Third, it appears from the plot that carbon dioxide has no particular affinity for the calcite interface, it is mostly spread evenly throughout the water. So one may conclude that whatever affected the excess surface energy of aqueous carbon-dioxide system compared to a pure water one, was actually water restructuring to accommodate carbon dioxide molecules. Carbon dioxide is a significantly larger molecule than water, so it does not fit into the calcite surface as water does. Figures 2 and 3 illustrate this effect quite well. Both VMD-generated views and density profiles suggest that the carbon dioxide does not have any affinity for the interface. They do not cluster either, but position themselves nearer to each other than to the interface.

4 Conclusions

We have applied the techniques of molecular simulations to study two surfaces of calcite mineral under dry and wet conditions. The wetting phase was presented either by pure water or water–carbon dioxide mixtures. Excess surface energies were estimated from the potential energies of interfacial and bulk systems. We have found that the results of our simulation involving relaxed calcite surfaces under vacuum and in contact with pure water are in compliance with experimentally observed morphology of calcite mineral. They are also mostly in good agreement with available literature findings, notable those of Hwang et al. [2]. This agreement supports our conclusion that the stability order of calcite cleaving surfaces under investigation will remain unchanged in the presence of water–carbon dioxide mixture as well. The structural features of calcite–fluid interface were analyzed with the help of density profiles using binning techniques and smoothing filters. The profiles are quite instructive and can offer insight into the effects that wetting has on the rearrangement of calcite surface.

References

1. W. Humphrey, A. Dalke, K. Schulten, VMD—visual molecular dynamics. J. Mol. Graph. **14**, 33–38 (1996)
2. S. Hwang, M. Blanco, E. Demiralp, T. Cagin, W.A. Goddard, The MS-Q force field for clay minerals: application to oil production. J. Phys. Chem. B **105**, 4122–4127 (2001)
3. S. Kerisit, S.C. Parker, J.H. Harding, Atomistic simulation of the dissociative adsorption of water on calcite surfaces. J. Phys. Chem. B **107**, 7676–7682 (2003)
4. M. Levitt, M. Hirshberg, R. Sharon, K.E. Ladig, V. Dagett, Calibration and testing of a water model for simulation of the molecular dynamics of proteins and nucleic acids in solution. J. Phys. Chem. B **101**, 5051–5061 (1997)
5. A.P. Lyubartsev, A. Laaksonen, M.DynaMix—a scalable portable parallel MD simulation package for arbitrary molecular mixtures. Comput. Phys. Commun. **128**, 565–589 (2000)
6. S.L. Mayo, B.D. Olafson, W.A. Goddard, Dreiding—a generic force-field for molecular simulations. J. Phys. Chem. **94**, 8897–8909 (1990)
7. M.I.H. Panhuis, C.H. Patterson, R.M.A Lynden-Bell, Molecular dynamics study of carbon dioxide in water: diffusion, structure and thermodynamics. Mol. Phys. **94**, 963–972 (1998)
8. S. Tsuzuki, K. Tanabe, Molecular dynamics simulations of fluid carbon dioxide using the model potential based on ab initio MO calculation. Comput. Mater. Sci. **14**, 220–226 (1999)
9. K. Wright, R.T. Cygan, B. Slater, Structure of the (10(1)over-bar4) surfaces of calcite, dolomite and magnesite under wet and dry conditions. PCCP, **3**, 839–844 (2001)